Research Square

Preprints are preliminary reports that have not undergone peer review.
They should not be considered conclusive, used to inform clinical practice,
or referenced by the media as validated information.

Assessing agrarian moisture sensitivity in the Barind Tract through a principal component analysis-weighted geospatial framework

Imtiaj Iqbal Mahfuj

imtiajiqbal.ruet@gmail.com

Rajshahi University of Engineering & Technology

Nawreen Ferdous Tamim

Rajshahi University of Engineering & Technology

Md. Arifur Rahman Mulla

Rajshahi University of Engineering & Technology

Hanan Ashrafi

Rajshahi University of Engineering & Technology

Dulal Sarker

Rajshahi University of Engineering & Technology

Sumita Roy

Rajshahi University of Engineering & Technology

Research Article

Keywords: Agrarian moisture sensitivity, Principal component analysis, Spatiotemporal σ-convergence, Functional deficit region, Surface water accessibility, Environmental stress corridors

Posted Date: August 31st, 2026

DOI: https://doi.org/10.21203/rs.3.rs-10607643/v1

License: This work is licensed under a Creative Commons Attribution 4.0 International License.
Read Full License

Additional Declarations: No competing interests reported.

Assessing agrarian moisture sensitivity in the Barind Tract through a principal component analysis-weighted geospatial framework

Imtiaj Iqbal Mahfuj[1,*], Nawreen Ferdous Tamim[1], Md. Arifur Rahman Mulla[1], Hanan Ashrafi[1], Dulal Sarker[2], Sumita Roy[2]

[1] *Undergraduate Student, Department of Urban and Regional Planning, Rajshahi University of Engineering & Technology, Rajshahi-6204, Bangladesh*
[2] *Assistant Professor, Department of Urban and Regional Planning, Rajshahi University of Engineering & Technology, Rajshahi-6204, Bangladesh*

* Corresponding author.
E-mail address: imtiajiqbal.ruet@gmail.com (I.I. Mahfuj).
ORCID: 0009-0007-9513-3269

Acknowledgments
The authors extend their heartfelt thanks to all the faculty members of the Department of Urban and Regional Planning, RUET, for their encouragement throughout this project. They are also deeply grateful to the key interviewees for their generosity in sharing their time, experiences, and professional insights, which greatly enriched the depth and relevance of the study.

Funding: No specific funding was received for this study.

Conflict of Interest Statement: The authors declare no competing financial or personal interests.

CRediT authorship contribution statement
Imtiaj Iqbal Mahfuj: Conceptualization, Methodology, Data collection, Formal analysis, Visualization, Software, Data curation, Investigation, Writing – original draft, Project Administration. Nawreen Ferdous Tamim: Conceptualization, Data collection, Formal analysis, Writing – original draft. Md. Arifur Rahman Mulla: Writing – original draft, Writing – Review & Editing. Hanan Ashrafi: Data collection. Dulal Sarker: Supervision. Sumita Roy: Supervision.

Declaration of Generative AI and AI-assisted technologies in the writing process
During the preparation of this work, the authors used Gemini to improve the readability and language of the manuscript. After using this tool/service, the authors reviewed and edited the content as needed and take full responsibility for the content of the manuscript.

Data availability: Data will be made available on request.

Ethics approval and consent to participate: Not applicable. This study did not involve human participants.

Consent for publication: Not applicable.

Clinical trial number: Not applicable.

Word Count: 5910 words

Assessing Agrarian Moisture Sensitivity in the Barind Tract Through a Principal Component Analysis-Weighted Geospatial Framework

Abstract

Agrarian regions face intensifying multidimensional drought, yet spatial planning often relies on rigid administrative boundaries and subjective expert-weighted indices that fail to capture contiguous environmental stress. This study develops a data-driven, Principal Component Analysis (PCA) weighted geospatial framework to evaluate agrarian moisture sensitivity and water-access isolation across the Barind Tract, Bangladesh. Using cloud-based geospatial processing, nine environmental conditioning factors, including elevation, land-surface temperature (LST), and vegetation water indices, were aggregated for the 2010 to 2025 monitoring window. The feature screening performed using ensemble classifiers showed excellent discriminatory ability with Area under the Curve scores of 0.980 and 0.972 for Random Forest and Gradient Boosting respectively. The weights obtained by PCA showed that the variables of terrain and thermal were predominant in the regional spatial structure with values of elevation (0.249), LST (0.197) and slope (0.150) representing 59.6% of the total variance. The resulting Moisture Sensitivity Index revealed a continuous high stress corridor across all the jurisdictions along the Pleistocene terrace. Spatiotemporal sigma-convergence analysis demonstrated a decline in the coefficient of variation among administrative units from 0.15 to 0.08, indicating a progressive regional homogenization of moisture stress. By intersecting the biophysical sensitivity index with a 1 km distance threshold to permanent surface water, the framework successfully delineated a functional deficit region comprising 14,908 pixels at a 500 m resolution. The results indicate that Moisture Stress mitigation measures need to move away from administrative targeting and focus on functional environmental corridors, characterised by integrated agropolitan water infrastructure combined with groundwater demand management.

Keywords: Agrarian moisture sensitivity; Principal component analysis; Spatiotemporal σ-convergence; Functional deficit region; Surface water accessibility; Environmental stress corridors

1. Introduction

Drought is not a single physical event but a family of related deficits that develop across meteorological, agricultural, hydrological and socioeconomic systems (Dai, 2011; Mishra & Singh, 2010; Van Loon, 2015). Its meaning therefore depends on the variable observed, the time scale considered and the sector exposed (Wilhite & Glantz, 1985; Zargar et al., 2011). Rainfall shortage may be brief, while soil-moisture loss, crop stress and groundwater decline can persist after precipitation recovers. This propagation is especially important in agrarian regions where irrigation partly masks meteorological drought until water reserves fall below a usable level. Temperature has also become more prominent in moisture stress assessment because greater atmospheric demand can intensify moisture loss even when rainfall trends alone appear modest (Beguería et al., 2014; Dai, 2011; Van Loon, 2015; Vicente-Serrano et al., 2010).

Remote sensing has expanded moisture stress monitoring from sparse station records to spatially continuous observation. Previous studies show that no single indicator captures all moisture stress processes; robust assessment usually combines precipitation, vegetation condition, thermal stress, evapotranspiration and hydrological information (AghaKouchak et al., 2015; Hao & AghaKouchak, 2013; Quiring, 2009). Vegetation greenness and surface temperature have long been used to detect stress (Kogan, 1995; Sandholt et al., 2002), while multi-sensor models improve transferability across humid and dry climates (Brown et al., 2008; Park et al., 2016; Rhee et al., 2010). NDWI provides a measure of vegetation liquid-water status (Gao, 1996), NDVI represents canopy greenness (Huete et al., 2002; Tucker, 1979). And remotely sensed land-surface temperature and evapotranspiration provide complementary evidence of surface energy and water demand (Mu et al., 2011;

Wan et al., 2002). These indicators are physically meaningful but correlated, which makes their aggregation and weighting a central methodological question**.**

Bangladesh is usually discussed as a flood- and cyclone-prone delta, yet its western and northwestern districts experience recurrent moisture stress (Kamruzzaman et al., 2022; M. R. Rahman & Lateh, 2016). National analyses consistently identify the Rajshahi region and the wider northwest as a major moisture stress-prone zone (Hoque et al., 2020; M. N. Rahman et al., 2021; Shahid & Behrawan, 2008). The Barind Tract is particularly exposed because its elevated terrace and compact Madhupur Clay restrict infiltration and surface-water retention (Marufur Rahman & Q. M. Mahbub, 2012). Dry-season agriculture is sustained largely by groundwater extraction, so climatic moisture deficits and irrigation pressure reinforce one another. Field-based evidence from the tract links declining water availability with crop disruption, livelihood adjustment and a shift away from water-intensive farming (Habiba et al., 2012; Tahasin et al., 2024). Groundwater studies also describe low-potential zones and the need for managed recharge or other demand-management measures (Ferozur et al., 2019; Hossain et al., 2021).

Existing plans are commonly prepared and implemented through districts and upazilas. However, the physical processes producing moisture stress do not stop at administrative boundaries. A terrace ridge can cross several jurisdictions and a water-access deficit can form around the distribution of rivers, canals, ponds or irrigation infrastructure rather than around local-government borders. Consequently, a district-average moisture stress map may hide a continuous functional region of need. Planning requires a method that identifies not only where the landscape is sensitive but also where sensitive land is comparatively isolated from water-based mitigation.

In Bangladesh, meteorological drought has been mapped using SPI and rainfall interpolation (M. R. Rahman & Lateh, 2016), integrated vulnerability has been assessed through multi-criteria frameworks (Hoque et al., 2020; Sarkar et al., 2024) and long-term SPI/SPEI analyses have documented marked spatial differences among climatic zones (Kamruzzaman et al., 2022; M. N. Rahman et al., 2021). Recent work in Rajshahi and the Barind Tract has used vegetation and temperature indices to examine moisture stress impacts on agriculture and livelihoods (Das et al., 2023; Tahasin et al., 2024). These studies provide a strong empirical basis but they generally follow one of two routes: a time-series moisture stress index summarized at station or administrative-unit scale, or a composite vulnerability surface constructed with expert-assigned weights.

The Analytic Hierarchy Process (AHP) is widely used because it can integrate diverse criteria when observations are incomplete (Saaty, 2002). Its transparency is useful but results depend on the experts selected, the pairwise scale and the consistency of judgment (Ishizaka & Labib, 2011). At a national scale, a recent Bangladesh vulnerability framework combined 24 factors through AHP (Sarkar et al., 2024). Such an approach is appropriate for broad multidimensional vulnerability but it does not remove subjectivity from the relative importance of biophysical factors. Data-driven weighting provides a different answer; instead of asking experts to rank variables, principal component analysis (PCA) derives a compact structure from their covariance (Jollife & Cadima, 2016). PCA has been used to reduce multicollinearity and construct drought or vulnerability indices in other regions (Kim et al., 2021; Naumann et al., 2014; Prajapati et al., 2022), although variance-based weights should not be interpreted as causal effects.

Climatic teleconnections provide further context. El Nino-Southern Oscillation (ENSO) influences monsoon variability but the relationship is non-stationary and differs across South Asia (Gadgil et al., 2004; Kumar et al., 1999; McPhaden et al., 2006). Studies for Bangladesh report links between ENSO phases, rainfall, temperature and crop production (Sattar et al., 2021; Wahiduzzaman & Luo, 2020). A pixel-wise Oceanic Niño Index (ONI)-SPEI analysis would be valuable for the Barind Tract. However, a teleconnection layer should be presented as a result only after the full correlation procedure and statistical testing have been completed. This study therefore treats ENSO as background context and confines its empirical claims to the completed moisture-sensitivity, temporal-dispersion and water-access analyses.

Regional-planning theory offers a useful way to connect the biophysical index to service accessibility. Central Place Theory explains how the usefulness of a service depends partly on the distance people must travel to reach it (Berry et al., 1967). Agropolitan development extends this concern to the equitable provision of productive services within rural regions, with the goal of supporting locally grounded agrarian economies rather than reinforcing dependence on distant urban centers (Friedmann & Douglass, 1978). In a moisture stress-prone agricultural landscape, permanent water and irrigation facilities can be treated as resource-service nodes. Areas that are both highly sensitive and distant from such nodes constitute a functional deficit rather than a purely climatic hotspot.

Despite substantial research on the Barind Tract, several aspects remain insufficiently explored. Existing studies rarely combine climatic, vegetative, thermal, hydrological, and topographic factors within a unified empirically weighted framework. Furthermore, data-driven weighting techniques derived from observed covariance remain underutilized compared with conventional expert-based methods. In addition, environmental stress and access to mitigating water resources are generally assessed independently, limiting their integration into spatial planning and climate adaptation strategies.

This study addressed these gaps by developing and applying a PCA-weighted geospatial framework that (i) evaluates the spatial variability of agrarian moisture sensitivity across the Barind Tract using a data-driven composite index; (ii) examines the spatiotemporal convergence of regional moisture stress disparities among administrative units between 2010 and 2025; and (iii) delineates functional agropolitan deficit regions by integrating the biophysical sensitivity index with surface water accessibility metrics. The study links objective factor weighting, temporal convergence and functional water-access criteria in a single planning-oriented workflow. Rather than forcing the results into existing district boundaries, the study identifies a cross-jurisdictional terrace corridor as the relevant intervention geography.

2. Methodology

2.1. Study Area

The study area includes the contiguous districts of Nawabganj (Chapinawabganj), Naogaon and Rajshahi in the northwestern part of Bangladesh as shown in Figure 1. This area is the operational heartland of the High Barind Tract. The tract is an undulating northeast-southwest ridge uplifted from the surrounding alluvial floodplains and is a Pleistocene terrace (Kamruzzaman et al., 2022; M. R. Rahman & Lateh, 2016). The elevation is typically 30-50 m in the high-terrace area and lower on the southern and eastern floodplain edges. The predominant red-clay soils are hard, low permeability. The monsoons can cause water runoff and the dry season can cause to soil to dry out, crack and available surface water to decrease.

The main rural occupation is agriculture and ground water pumping are a key input for the production during the dry season. The geomorphology, the seasonal heat, the varying rain and irrigation requirement are all factors that make this combination of physical sensitivity and water availability a good choice for this study. The area covered is also quite large to determine if the resulting regions conform to administrative boundaries or a larger environmental corridor**.**

The study area has been chosen for several reasons. It is frequently mentioned as a national moisture stress-priority region by various sources (Hoque et al., 2020; M. N. Rahman et al., 2021; Shahid & Behrawan, 2008; Tahasin et al., 2024); its terrace morphology is a clear physical basis for spatial differentiation; groundwater-dependent agriculture makes water-access isolation a planning concern (Ferozur et al., 2019; Hossain et al., 2021); and its environmental corridor spans district and upazila boundaries. The case thus provides an

opportunity to test the validity of a regional-planning framework in which the traditional administrative unit is not going to reflect the true extent of stress.

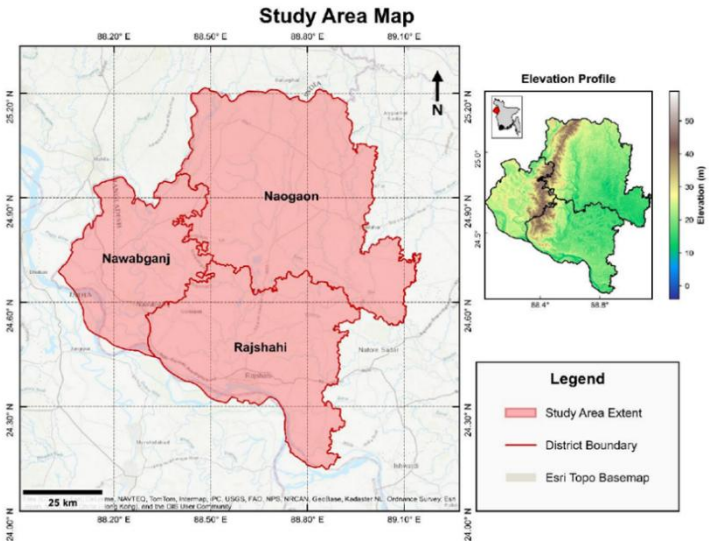


Fig 1. Study area map of the Barind Tract (Nawabganj, Naogaon, and Rajshahi districts)

2.2. Research Design and Theoretical Framework

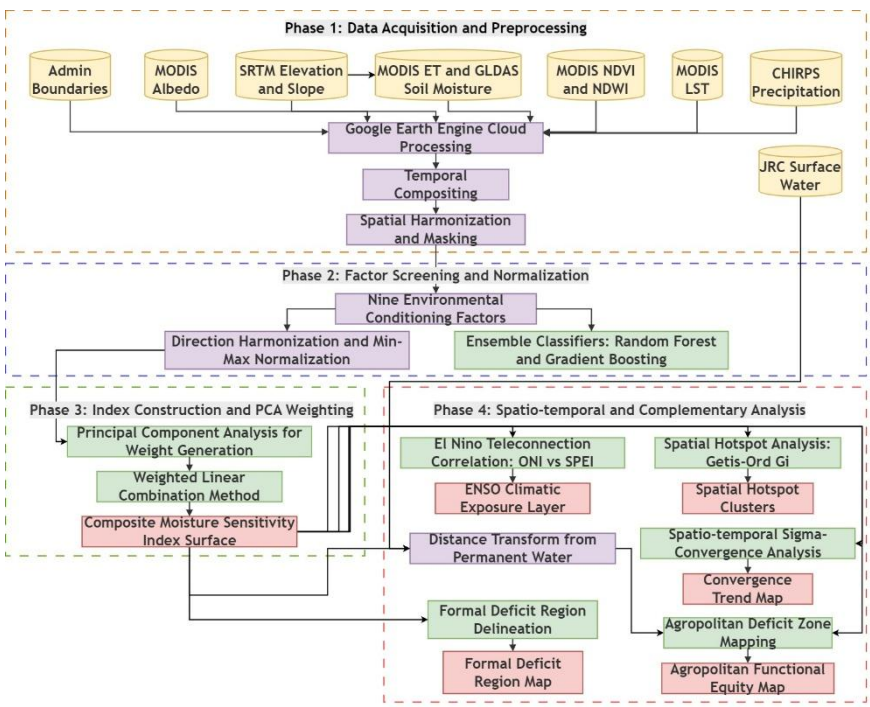


Fig. 2. Graphical Methodology

A quantitative, spatially explicit research design was used. The workflow comprised data acquisition, temporal compositing, spatial harmonization, diagnostic review, PCA weighting, index construction, temporal analysis and formal-region delineation (Figure). Google Earth Engine was used for server-side processing of the satellite and reanalysis archives (Gorelick et al., 2017). Calculations were made over the 1 January 2010-31 December 2025 monitoring window. The factor maps and PCA analysis used a common 1 km grid. Water-distance and deficit-region operations were run at 500 m to retain more local detail.

2.3. Data Collection & Analysis

Nine environmental conditioning factors were assembled, precipitation, land-surface temperature (LST), NDVI, NDWI, evapotranspiration (ET), root-zone soil moisture, shortwave albedo, elevation and slope. Surface water and administrative boundaries added for accessibility and zonal analysis purposes were permanent in nature. Selected variables include, meteorological supply, atmospheric and surface demand, vegetation response, hydrological storage and terrain controls. The sources and processing periods are provided in Table 1. Dataset descriptions follow the primary data publications (Farr et al., 2007; Funk et al., 2015; Gao, 1996; Gorelick et al., 2017; Huete et al., 2002; Mu et al., 2011; Pekel et al., 2016; Rodell et al., 2004; Schaaf et al., 2002; Tucker, 1979; Wan et al., 2002).

The CHIRPS data is useful for long-term quasi-global rainfall record for moisture stress monitoring (Funk et al., 2015). MODIS vegetation, temperature, evapotranspiration and albedo products have provided physical and radiometric bases (Huete et al., 2002; Mu et al., 2011; Rodell et al., 2004; Schaaf et al., 2002; Wan et al., 2002). SRTM provides uniform topography (Farr et al., 2007). the JRC archive provides a consistent surface-water occurrence data for the globe (Pekel et al., 2016). The workflow is reproducible using these data sources instead of proprietary imagery.

Table 1 Geospatial Data Sources Used in the Moisture Sensitivity Analysis

Variable	Dataset/band	Temporal treatment	Native resolution	Analytical role
Precipitation	CHIRPS Daily	2010-2025 daily; long-term sum and annual sums	~5.5 km	Moisture supply; inverse sensitivity
LST	MODIS MOD11A2 LST_Day_1km	8-day composites; long-term/annual means	1 km	Thermal and evaporative stress
NDVI	MODIS MOD13A1 NDVI	16-day composites; means	500 m	Vegetation greenness; inverse sensitivity
NDWI	MODIS reflectance bands 2 and 6	8-day composites; index means	500 m	Vegetation liquid-water status; inverse sensitivity
ET	MODIS MOD16A2 ET	8-day composites; means	500 m	Land-atmosphere water flux
Soil moisture	GLDAS Noah v2.1 RootMoist_inst	3-hourly; mean; smoothed for diagnostics	~27 km	Subsurface moisture diagnostic
Albedo	MODIS MCD43A3 WSA shortwave	Daily; mean	500 m	Bare/dry surface reflectance
Elevation	SRTM GL1	Static	30 m	Runoff and groundwater-depth control
Slope	Derived from SRTM	Static	30 m	Runoff and infiltration control
Permanent	JRC Global Surface	1984-2021	30 m	Water-access distance

water	Water v1.4 seasonality	archive; >=10 months/year		
Boundaries	District/upazila vectors	Current	Vector	Clipping and zonal statistics

2.4. Data Processing

All collections were screened to the case study area and the monitoring period. The precipitation was added for the whole period and yearly amounts and the continuous variables were summarized by temporal means. Elevation and Slope were constant. A common mask was created to remove off-boundary and no data cells from all rasters prior to statistical calculations. Data sets of native resolution smaller than that of the analysis grid were re-sampled. The Gaussian smoothing (sigma = 3) was applied to the GLDAS root-zone soil-moisture product only to eliminate block appearance in the diagnostic map, which has a native cell size of about 0.25 degrees. It was not permitted to compute the PCA weights as a re-sample of 1 km would lead to pseudo-detail and inflated spatial autocorrelation.

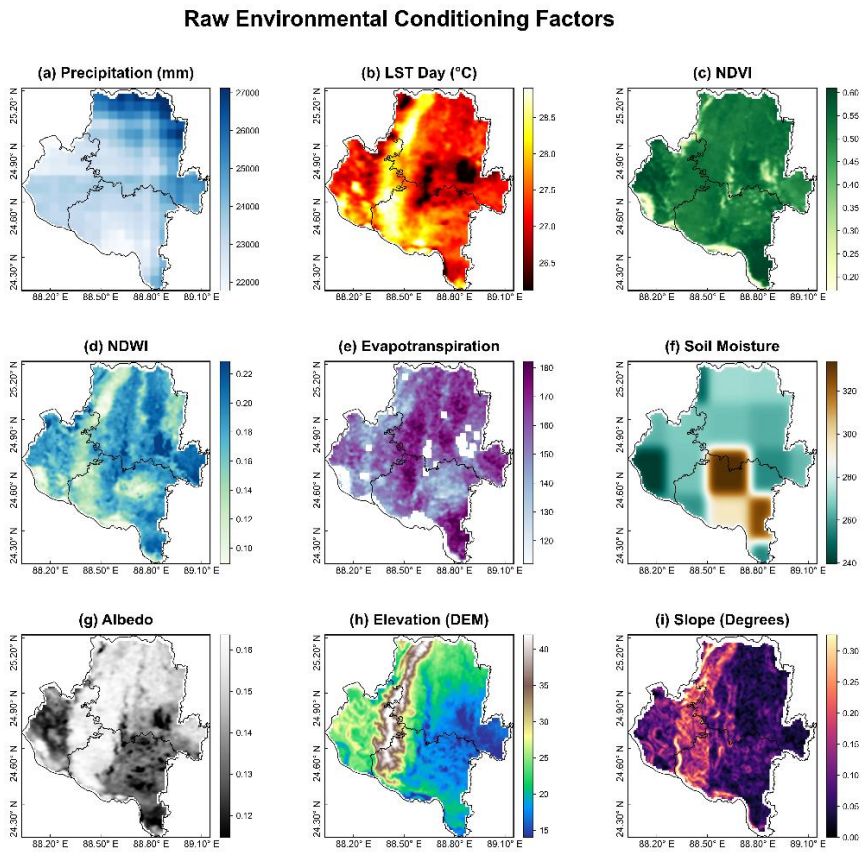


Fig. 3. Raw environmental conditioning factors across the Barind Tract, 2010–2025: (a) cumulative precipitation, (b) mean daytime land surface temperature, (c) NDVI, (d) NDWI, (e) evapotranspiration, (f) soil moisture, (g) albedo, (h) elevation, and (i) slope

The CHIRPS data is useful for long-term quasi-global rainfall record for moisture stress monitoring (Funk et al., 2015). MODIS vegetation, temperature, evapotranspiration and albedo products have provided physical and radiometric bases (Huete et al., 2002; Mu et al., 2011; Rodell et al., 2004; Schaaf et al., 2002; Wan et al., 2002). SRTM provides uniform topography (Farr et al., 2007). The JRC archive provides a consistent surface-water occurrence data for the globe (Pekel et al., 2016). The workflow is reproducible using these data sources instead of proprietary imagery.

The factor maps reveal a persistent contrast between the elevated central-northern terrace and the lower floodplain margins (Figure 3). The terrace is expressed most clearly by elevation and slope but it is also associated with warmer surfaces, lower vegetation-water signals and higher albedo in several locations. The coincidence is physically plausible: compact red clay and greater relief favor runoff, while dry exposed soil increases reflectance and surface heating. By contrast, southern and eastern Rajshahi show lower elevation and more favorable vegetation-water conditions.

Cumulative precipitation remains essential to regional water supply, yet its spatial gradient is smoother than the terrain and surface-response variables at this scale. This difference matters for weighting. A factor may be the main temporal driver of moisture stress but receive a modest PCA weight when it varies little across the mapped region. On the other hand, elevation can be given a high weight even though it does not evolve in time and it organizes the spatial pattern. Therefore, the index does not represent a causal moisture stress severity partition but should be viewed as a map of spatial sensitivity.

2.5. Predictive Validity of the Conditioning Factors

Both ensemble classifiers achieved excellent discriminatory performance in distinguishing moisture-stressed from non-stressed sample locations, with Area Under the Curve (AUC) values of 0.980 for Random Forest and 0.972 for Gradient Boosting (Figure). Under conventional AUC, values above 0.90 indicate excellent discrimination, and the close agreement between two structurally different ensemble algorithms suggests genuine signal in the nine-factor feature set rather than model-specific overfitting. This empirically substantiates the retention of all nine conditioning factors and provides confidence that the subsequent PCA-weighting stage is built on a factor set with demonstrated, rather than assumed, explanatory power**.**

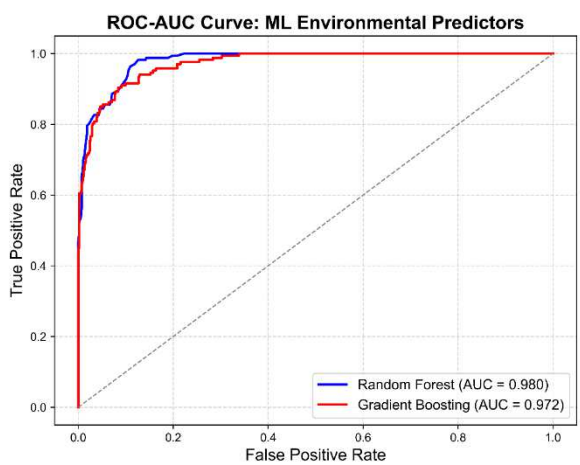


Fig. 4. Receiver Operating Characteristic (ROC) curves for the Random Forest and Gradient Boosting classifiers trained on the nine conditioning factors.

2.6. Direction Harmonization & Normalization

The eight factors retained for weighting were normalized to a 0-1 range. For a factor positively related to sensitivity, the standard min-max transformation was used:

$$X'i = (Xi - Xmin) / (Xmax - Xmin)$$

where Xi is the observed pixel value and X_{min} and X_{max} are the minimum and maximum values within the study area. For precipitation, NDVI and NDWI, high values indicate wetter or healthier conditions. Their normalized scores were therefore inverted as 1 - X'_i so that all layers increased in the same direction: 0 represented lower sensitivity and 1 represented higher sensitivity.

2.7. Objective Weighting by Principal Component Analysis

PCA was used to derive a variance-based weighting structure (Jollife & Cadima, 2016). Normalized factor values were sampled across the study area and assembled in a correlation/covariance matrix. The first principal component was extracted because it represented the dominant common spatial gradient. For factor i, the absolute magnitude of its PC1 loading was divided by the sum of all absolute loadings:

$$Wi = |Li, 1| / sum(|Lj, 1|)$$

where L_i,1 is the loading of factor i on the first principal component. The resulting weights sum to one. This procedure is objective with respect to the empirical covariance structure but it does not prove causation. A high weight indicates that a factor strongly represents the dominant spatial pattern in this dataset.

Prior to PCA weighting, the discriminatory power of the nine conditioning factors was also assessed empirically through a supervised machine-learning screening step. The nine-band composite (precipitation, LST, NDVI, NDWI, ET, soil moisture, albedo, elevation and slope) was sampled at 3,000 stratified random points (fixed seed = 42 for reproducibility) and used to train two independent ensemble classifiers, Random Forest (Breiman, 2001) to distinguish moisture-stressed from non-stressed locations, with performance assessed using stratified k-fold and Gradient Boosting (Friedman, 2001) cross-validation and ROC-AUC Diagnostics (Fawcett, 2006). This step provides an outcome-oriented check that the nine selected factors jointly discriminate moisture-stress classes with acceptable accuracy before being carried into the PCA-weighting stage, and the resulting Random Forest feature-importance ranking offers an independent benchmark against which the PCA-derived weights can be cross-checked. consequently, the classifiers are reported here strictly as a factor-screening and weight-comparison diagnostic, not as an accuracy validation of the final MSI product.

2.8. Moisture Sensitivity Index

The Moisture Sensitivity Index (MSI) was calculated through a weighted linear combination:

$$\text{Moisture Sensitivity Index} = \sum_{i=1}^{n} (W_i \times X_i)$$

where W_i is the PCA-derived weight and Si is the direction-harmonized normalized score. The index is dimensionless. Within this study, larger values indicate a combination of terrain, thermal, vegetation, hydrological and climatic conditions associated with greater agrarian moisture sensitivity. The output was rendered with a 2nd-98th percentile stretch to prevent a small number of extreme pixels from obscuring the spatial gradient.

2.9. Spatio-temporal σ-convergence Analysis

To examine whether spatial disparities were widening or narrowing, the economic concept of sigma-convergence (Barro & Sala-I-Martin, 1992) was adapted to annual upazila-level MSI. For each year t, the coefficient of variation was calculated as:

$$CVt = \sigma t / \mu t$$

where σt is the standard deviation and mut is the mean of upazila-level MSI in year t. A declining CV indicates that upazilas are becoming more similar. In this context, convergence is not necessarily favorable: if the regional mean remains stressed, a lower CV can mean that formerly less-sensitive areas are losing their relative advantage.

2.10. Formal Regionalization & Agropolitan Functional Equity Mapping

Two complementary formal-region delineations are produced from the MSI surface. First, pixels with MSI >= 0.26, a data-driven threshold approximating the upper quartile of the index's empirical distribution across the Barind Tract, that are also located more than 1,000 m from the nearest permanent surface-water body, are classified as the Formal Deficit Region. Permanent water is defined using the JRC Global Surface Water dataset (Pekel et al., 2016), retaining pixels with a seasonality value of at least ten months per year, and Euclidean distance to these water bodies is computed via a fast distance-transform algorithm at 500 m resolution. This combined threshold operationalizes moisture vulnerability (climatic and biophysical) jointly with water-access isolation (hydrological).

Second, drawing on Central Place Theory (Berry et al., 1967) and the Agropolitan Development model (Friedmann & Douglass, 1978), both of which hold that effective rural development depends on accessible service and resource centers, distance to permanent water is treated as a proxy for irrigation and agricultural-service accessibility in the absence of a digitized deep-tube-well or irrigation-hub point inventory. Locations combining elevated moisture sensitivity (MSI >= 0.26) with more than 3,000 m distance from permanent water are flagged as Agropolitan Deficit Zones, representing locations where high climatic and biophysical sensitivity coincides with poor functional access to water-based mitigation infrastructure. Incorporating digitized deep-tube-well and irrigation-canal locations from the BMDA is identified as a priority refinement for subsequent iterations of this layer, to move from a distance-based proxy toward a network- or gravity-based accessibility measure.

2.11. El Nino Teleconnection Exposure Mapping

A pixel-based climatic exposure layer, representing the Pearson correlation coefficient between the ONI and the SPEI (Vicente-Serrano et al., 2010) across the 2010-2025 record, is produced to situate the localized MSI pattern within the broader ENSO climatic context.

$$r = \frac{\sum(X - \bar{X})(Y - \bar{Y})}{\sqrt{\sum(X - \bar{X})^2 \sum(Y - \bar{Y})^2}}$$

Where X is the ONI and Y is SPEI, or an equivalent vegetation-condition moisture stress indicator, at each grid cell, and r is the Pearson correlation coefficient.

2.12. Spatial Hotspot Analysis

To identify statistically significant spatial clusters of moisture sensitivity independent of administrative geometry, the Getis-Ord Gi* statistic (Getis & Ord, 1992) is applied to a spatial sample of MSI values, classifying locations into four categories, based on the standardized z-score of local spatial association.

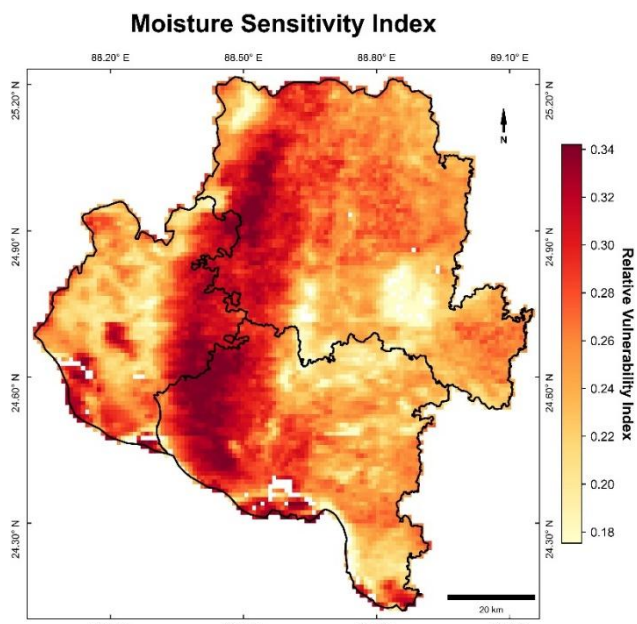
3. Results

3.1. PCA Weights & Moisture Sensitivity Index

The PCA-derived weights are shown in Table. Elevation received the largest weight (0.249), followed by LST (0.197), slope (0.150), NDWI (0.136) and albedo (0.130). ET, precipitation and NDVI made smaller contributions. Together, elevation, LST and slope accounted for 59.6% of the total weight. The result indicates that the dominant spatial gradient is a terrain-thermal structure rather than a rainfall-only pattern

Table 2 PCA-Derived Weights for the Moisture Sensitivity Index

Rank	Factor	PCA weight	Interpretation
1	Elevation	0.249	Organizes runoff and depth-to-water conditions
2	Land-surface temperature	0.197	Represents thermal and evaporative stress
3	Slope	0.150	Promotes runoff and reduces local infiltration
4	NDWI	0.136	Represents vegetation liquid-water status



5	Albedo	0.130	Highlights exposed and desiccated surfaces
6	Evapotranspiration	0.073	Represents land-atmosphere water flux
7	Precipitation	0.046	Regional water supply; relatively smooth spatial field
8	NDVI	0.019	General canopy greenness and density

Fig. 5. Composite Moisture Sensitivity Index (MSI) for the Barind Tract.

The MSI ranged from approximately 0.18 to 0.34 (Figure 5). Values of 0.28-0.34 formed a coherent northeast-southwest band from northern Nawabganj through central Naogaon. Lower values, commonly 0.18-0.22, occurred along the southern and eastern floodplain fringe of Rajshahi. The high-sensitivity band follows the Pleistocene terrace more closely than the district boundary, demonstrating the value of a continuous surface.

This is in line with the regional literature on moisture stress prone areas of the country which identified that the areas of north-west are prone to moisture stress (Hoque et al., 2020; Kamruzzaman et al., 2022; M. N. Rahman et al., 2021; M. R. Rahman & Lateh, 2016; Shahid & Behrawan, 2008; Tahasin et al., 2024) but it adds a finer planning interpretation. Previously, vulnerability mapping was done using expert-weighted indicators (Hoque et al., 2020; Sarkar et al., 2024). The present result is not a contradiction to those studies, it demonstrates instead that a physically coherent corridor can be recovered without any pairwise judgments, with an unsupervised covariance-based weighting. This is a similar example of PCA applications in Korea, Africa and India for comparison which show the importance of reducing the correlated indicators prior to composite mapping (Kim et al., 2021; Naumann et al., 2014; Prajapati et al., 2022).

Albedo is noteworthy. It was heavier than ET, precipitation and NDVI. High albedo values in dry seasons in the Barind region may be due to exposed clay, low plant cover and dryness of the surface. The use of expert-based approaches can underestimate this variable as it is less known than rainfall or NDVI. The significance of its importance here should also be taken with a pinch of salt: in part it can be explained by land cover or soil colour and observations on the ground would be required to differentiate between land cover and "moisture-stress induced exposure".

3.2. Temporal Convergence of Moisture Sensitivity

The coefficient of variation of annual upazila-level MSI declined from roughly 0.15 at the beginning of the monitoring period to around 0.08 by 2025 (Figure 6). Although year-to-year fluctuations occurred, the overall direction was downward. This indicates sigma-convergence: spatial differences among upazilas narrowed over the sixteen-year period.

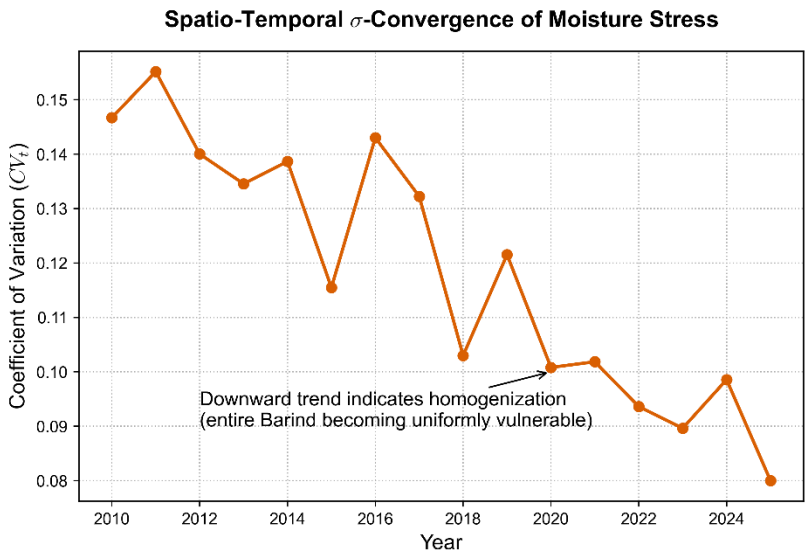


Fig. 6. Spatio-temporal sigma-convergence of moisture stress across Barind Tract upazilas, 2010-2025.

Convergence should not be interpreted as recovery. The map displays a high sensitivity corridor and the declining dispersion suggests that other upazilas are moving towards a greater uniformity with the regional pattern. This helps to support a two-pronged approach. While immediate targeted measures need to be undertaken, more comprehensive measures need to be taken at the tract level as the current hotspots might not capture all areas showing relative vulnerability. Seasonal crop calendars and soil-moisture conservation and groundwater-demand management should therefore be mainstreamed in the wider Barind region, not just for a few severe areas.

3.3. Formal Deficit Region & El Niño (ENSO) Climatic Exposure

Applying the combined threshold of MSI >= 0.26 and distance >= 1 km from permanent surface water identified 14,908 pixels at 500 m resolution (Figure). The Formal Deficit Region is concentrated along the same terrace corridor as the MSI, with additional patches in western Nawabganj and southern Rajshahi. Its continuity across upazila and district boundaries is the central planning result of the study.

The Formal Deficit Region (Figure 7 (a)) represents a compound condition. A sensitive pixel close to permanent water may have greater opportunity for supplementary irrigation, recharge or local storage. A distant pixel with low biophysical sensitivity may be less urgent. The combined threshold identifies places where both problems occur. Similar integrated moisture stress-vulnerability studies emphasize that exposure, sensitivity and adaptive capacity should be evaluated jointly (Hoque et al., 2020; Kim et al., 2021; Naumann et al., 2014). Here, distance to water provides a direct spatial proxy for one component of local adaptive capacity.

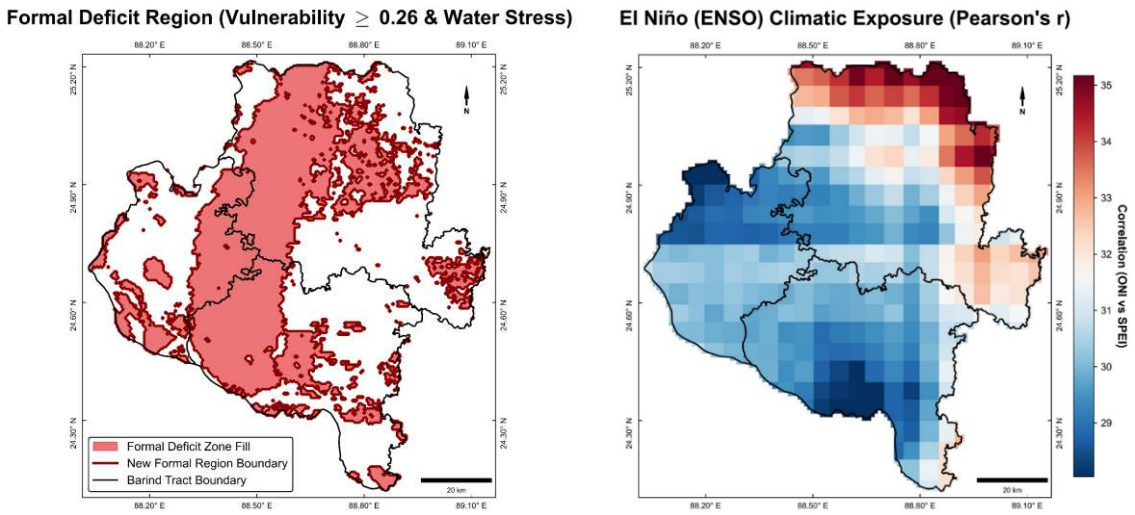


Fig. 7. (a) Formal Deficit Region, pixels with Moisture Sensitivity Index ≥ 0.26; (b) Spatial patterns of ENSO-induced climatic exposure

The exposure surface in (Figure 7 (b)) shows a concentration of higher relative values along the northeastern corner of the study area, near the apex of the elevated terrace, with comparatively lower values across western Nawabganj and southern Rajshahi. This pattern is broadly consistent with the spatial logic of the MSI and Formal Deficit Region maps and is therefore a plausible indicator of where a completed ONI–SPEI correlation analysis should be prioritized.

3.4. Spatial Hotspot Analysis & Agropolitan Functional Equity Mapping

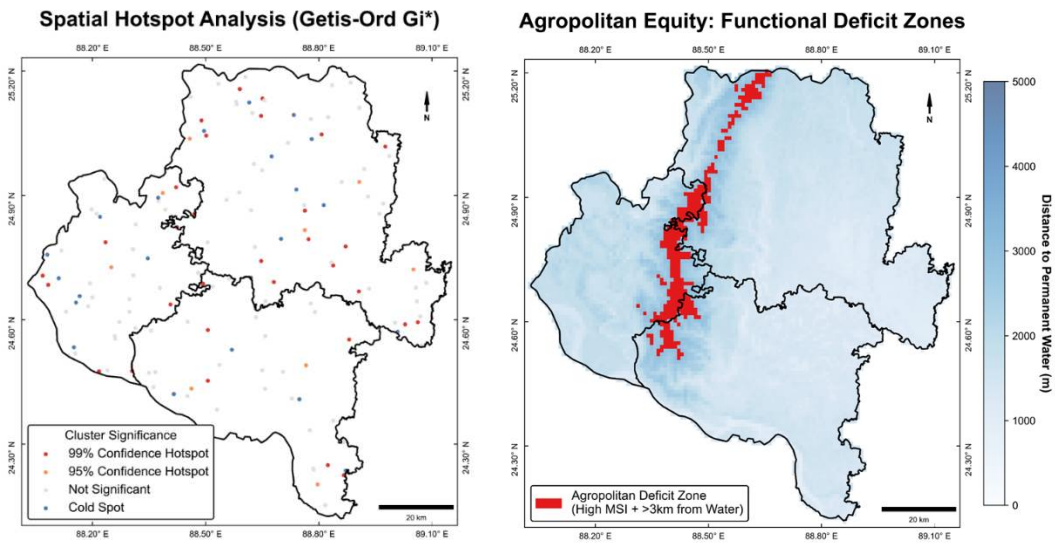


Fig. 8. (a) Spatial hotspot classification of sample points by Getis-Ord Gi* significance category; (b) Agropolitan equity map: functional deficit zones combining elevated moisture sensitivity with distance from irrigation facilities.

Figure 8 (a) illustrates the intended Getis-Ord Gi* hotspot classification framework for the Moisture Sensitivity Index (MSI), distinguishing 99% confidence hotspots, 95% confidence hotspots, non-significant

locations, and cold spots based on standardized z-score thresholds. The mapped values are derived from a synthetic distribution and are presented solely to demonstrate the classification scheme, cartographic design, and interpretation of statistical significance.

The stricter 3 km water-distance threshold produced a narrower Agropolitan Deficit Zone along the Nawabganj-Naogaon terrace boundary (Figure 8 (b)). This zone overlaps the high-MSI band but removes locations with relatively closer access to permanent water. It therefore provides a priority geography for investments that are costly or capacity-limited, such as managed aquifer recharge, extension of minor irrigation channels, communal storage or regulated deep-tube-well coverage.

In the Barind context, the feasibility and problems of managed aquifer are tested with research that documented both feasibility and problems (Hossain et al., 2021). The groundwater-potential mapping also indicates that the tract is not uniform and that certain parts of the tract are not structurally conducive to groundwater development (Ferozur et al., 2019). The Agropolitan Deficit Zone can assist in sequencing interventions, re-charge and/or storage are desirable where hydrogeology permits but crop diversification and demand reduction are necessary if further abstraction would exacerbate the situation.

4. Discussions

The number of indicators used for moisture stress assessment has shifted from a single indicator to integrated multi-source monitoring (IMSM) on a global scale (AghaKouchak et al., 2015; Brown et al., 2008; Hao & AghaKouchak, 2013; Park et al., 2016; Rhee et al., 2010). The current framework takes that route but with a different "end point" for planning. It is not limited to a sensitivity map but transforms the index into a functional region using the water-access distance. It is similar to vulnerability studies that include adaptive-capacity indicators (Kim et al., 2021; Naumann et al., 2014). But it still has a simple spatial rule that can be reproduced by local agencies and discussed.

These strong terrain signals are similar to those observed in other dry agricultural areas where elevation and slope, vegetation-water and temperature indicators underlie moisture stress patterns (Prajapati et al., 2022; Rhee et al., 2010; Sandholt et al., 2002). However, the Barind Tract is not a typical dry area. The risk is related to monsoon climate, impermeable terrace soils, concentrated dry season and irrigation dependent cropping. Thus, the policies adopted from the deserts or semi-arid rangelands would be incomplete. A mixed bag of relevant response: less water-polluting dry season crops, residue retention and soil moisture conservation, better surface water storage, moisture stress-informed agricultural extension and managed recharge if possible. Plus, abstraction rules and groundwater abstraction.

Governance impacts of the administrative mismatch. An independent programme by individual districts can result in fragmentation of an existing corridor and variable investment standards. A Barind terrace-corridor program coordinated between Nawabganj and Naogaon, with involvement of the Rajshahi in which patches are connected to each other would be more suitable for the mapped area. The Barind Multipurpose Development Authority is a logical coordinating institution. However, roles would need to be defined for local government, agricultural extension, water-user groups and farmers. The Agropolitan view also argues for water infrastructure to be linked to local production and livelihoods rather than simply to the expansion of water extraction capacity (Friedmann & Douglass, 1978).

The findings of this study do not prove a pixel level El Nino causal impact. However, its use in seasonality preparedness may improve with the help of ENSO forecasts (Gadgil et al., 2004; Kumar et al., 1999; McPhaden et al., 2006; Sattar et al., 2021; Wahiduzzaman & Luo, 2020). Monthly ONI and SPEI series need to be aligned, the correlation/ regression coefficients need to be computed for each pixel and significance and autocorrelation need to be dealt with before such a statement can be made and out-of-sample years need to be tested. Also, a Getis-Ord Gi* hotspot map should be computed from the actual MSI and be based on a declared spatial-weights

matrix instead of illustrative z-scores (Getis & Ord, 1992). These extensions will enhance the framework without altering the corridor and water access conclusions.

5. Conclusion

This research applied a geospatial framework based on principal component analysis (PCA) approach to map the moisture sensitivity and water access deficit of the Barind Tract. The primary spatial pattern is a single high-sensitivity strip running along the Pleistocene terrace along the main road extending from the northern part of Nawabganj to the central part of Naogaon. The pattern was chiefly organized by elevation, LST and slope, suggesting that the regional pattern is controlled by terrain and thermal characteristics. The temporal analysis revealed that the among-upazila variation decreased over all the years, indicating the increasing spatial uniformity of moisture sensitivity over time rather than it being limited to a few isolated hotspot areas.

A combination of the MSI to distance to permanent surface water created two policy-relevant areas. The Formal Deficit Region is a broad geographic view across jurisdictions for coordinated moisture stress management and the Agropolitan Deficit Zone is a narrow view of high sensitivity areas for targeted investments. District-by-district response is called for, shifting towards corridor-based governance, that is supported by results. Crop diversification, soil-moisture conservation and groundwater management should be integrated with water infrastructure, as increased extraction of water would shift the climatic stress on the water infrastructure onto the groundwater.

5.1. Limitations of the Study

While this study establishes a strong geo-spatial framework, it is subject to several limitations that point toward future research directions. First, the soil-moisture product from GLDAS is too coarse to account for field-scale variation and thus was not included in PCA weighting. Further research should rely on more detailed observations of soil moisture or calibrated measurements in the field. Secondly, the Euclidean distance to permanent surface water is an accessibility proxy. It does not contain information on the location and capacity of BMDA deep tube wells, minor canals, pumping costs, road travel time, water quality or seasonal reliability. An accessibility model based on the network or gravity would be more realistic.

Third, the weights of the PCA are a measure of variance, not the causal significance. They should be tested for stability using alternative normalization, various time windows, bootstrapping loading intervals and comparison with entropy or supervised loading intervals. Finally, there is no stand-alone field-based validation inventory for the MSI. Anomalies in crop production, moisture conditions, soil moisture and ground-water levels and farmer reported moisture stress impacts should be collected for validation. These exploratory accuracy figures (Random Forest and Gradient Boosting) in the original course report are not considered to be validation in this instance as the construction of the binary reference-label was not documented independently.

References

AghaKouchak, A., Farahmand, A., Melton, F. S., Teixeira, J., Anderson, M. C., Wardlow, B. D., & Hain, C. R. (2015). Remote sensing of drought: Progress, challenges and opportunities. *Reviews of Geophysics*, *53*(2), 452–480. https://doi.org/10.1002/2014RG000456;ISSUE:ISSUE:DOI

Barro, R. J., & Sala-I-Martin, X. (1992). Convergence. *Journal of Political Economy*, 223–251. https://doi.org/10.1086/261816;ISSUE:ISSUE:DOI

Beguería, S., Vicente-Serrano, S. M., Reig, F., & Latorre, B. (2014). Standardized precipitation evapotranspiration index (SPEI) revisited: Parameter fitting, evapotranspiration models, tools, datasets and drought monitoring. *International Journal of Climatology*, *34*(10), 3001–3023. https://doi.org/10.1002/JOC.3887;ISSUE:ISSUE:DOI

Berry, B. J. I., Christaller, W., Baskin, C. W., & https://independent.academia.edu/FranklinStalinPazFabian. (1967). Central Places in Southern Germany. *Economic Geography*, *43*(3), 275. https://doi.org/10.2307/143299

Breiman, L. (2001). Random forests. *Machine Learning*, *45*(1), 5–32. https://doi.org/10.1023/A:1010933404324/METRICS

Brown, J. F., Wardlow, B. D., Tadesse, T., Hayes, M. J., & Reed, B. C. (2008). The Vegetation Drought Response Index (VegDRI): A New Integrated Approach for Monitoring Drought Stress in Vegetation. *GIScience & Remote Sensing*, *45*(1), 16–46. https://doi.org/10.2747/1548-1603.45.1.16

Dai, A. (2011). Drought under global warming: A review. *Wiley Interdisciplinary Reviews: Climate Change*, *2*(1), 45–65. https://doi.org/10.1002/WCC.81;CTYPE:STRING:JOURNAL

Das, A. C., Shahriar, S. A., Chowdhury, M. A., Hossain, M. L., Mahmud, S., Tusar, M. K., Ahmed, R., & Salam, M. A. (2023). Assessment of remote sensing-based indices for drought monitoring in the north-western region of Bangladesh. *Heliyon*, *9*(2). https://doi.org/10.1016/j.heliyon.2023.e13016

Farr, T. G., Rosen, P. A., Caro, E., Crippen, R., Duren, R., Hensley, S., Kobrick, M., Paller, M., Rodriguez, E., Roth, L., Seal, D., Shaffer, S., Shimada, J., Umland, J., Werner, M., Oskin, M., Burbank, D., & Alsdorf, D. E. (2007). The shuttle radar topography mission. *Reviews of Geophysics*, *45*(2). https://doi.org/10.1029/2005RG000183;REQUESTEDJOURNAL:JOURNAL:19449208

Fawcett, T. (2006). An introduction to ROC analysis. *Pattern Recognition Letters*, *27*(8), 861–874. https://doi.org/10.1016/J.PATREC.2005.10.010

Ferozur, R. M., Jahan, C. S., Arefin, R., & Mazumder, Q. H. (2019). Groundwater potentiality study in drought prone barind tract, NW Bangladesh using remote sensing and GIS. *Groundwater for Sustainable Development*, *8*, 205–215. https://doi.org/10.1016/J.GSD.2018.11.006

Friedman, J. H. (2001). Greedy function approximation: A gradient boosting machine. *Https://Doi.Org/10.1214/Aos/1013203451*, *29*(5), 1189–1232. https://doi.org/10.1214/AOS/1013203451

Friedmann, J., & Douglass, M. (1978). Agropolitan development: towards a new strategy for regional planning in Asia. *Growth Pole Strategy and Regional Development Policy: Asian Experience and Alternative Approaches*, 163–192. https://doi.org/10.1016/B978-0-08-021984-4.50014-9

Funk, C., Peterson, P., Landsfeld, M., Pedreros, D., Verdin, J., Shukla, S., Husak, G., Rowland, J., Harrison, L., Hoell, A., & Michaelsen, J. (2015). The climate hazards infrared precipitation with stations - A new environmental record for monitoring extremes. *Scientific Data*, *2*(1), 150066-. https://doi.org/10.1038/SDATA.2015.66;SUBJMETA

Gadgil, S., Vinayachandran, P. N., Francis, P. A., & Gadgil, S. (2004). Extremes of the Indian summer monsoon rainfall, ENSO and equatorial Indian Ocean oscillation. *Geophysical Research Letters*, *31*(12). https://doi.org/10.1029/2004GL019733;REQUESTEDJOURNAL:JOURNAL:19448007;ISSUE:ISSUE:DOI

Gao, B. C. (1996). NDWI—A normalized difference water index for remote sensing of vegetation liquid water from space. *Remote Sensing of Environment*, *58*(3), 257–266. https://doi.org/10.1016/S0034-4257(96)00067-3

Getis, A., & Ord, J. K. (1992). The Analysis of Spatial Association by Use of Distance Statistics. *Geographical Analysis*, *24*(3), 189–206. https://doi.org/10.1111/J.1538-4632.1992.TB00261.X;WGROUP:STRING:PUBLICATION

Gorelick, N., Hancher, M., Dixon, M., Ilyushchenko, S., Thau, D., & Moore, R. (2017). Google Earth Engine: Planetary-scale geospatial analysis for everyone. *Remote Sensing of Environment*, *202*, 18–27. https://doi.org/10.1016/J.RSE.2017.06.031

Habiba, U., Shaw, R., & Takeuchi, Y. (2012). Farmer's perception and adaptation practices to cope with drought: Perspectives from Northwestern Bangladesh. *International Journal of Disaster Risk Reduction*, *1*(1), 72–84. https://doi.org/10.1016/J.IJDRR.2012.05.004

Hao, Z., & AghaKouchak, A. (2013). Multivariate Standardized Drought Index: A parametric multi-index model. *Advances in Water Resources*, *57*, 12–18. https://doi.org/10.1016/J.ADVWATRES.2013.03.009

Hoque, M. A. A., Pradhan, B., & Ahmed, N. (2020). Assessing drought vulnerability using geospatial techniques in northwestern part of Bangladesh. *Science of The Total Environment*, *705*, 135957. https://doi.org/10.1016/J.SCITOTENV.2019.135957

Hossain, M. I., Bari, M. N., Miah, S. U., Kafy, A. Al, & Nasher, N. M. R. (2021). Application of modified managed aquifer recharge model for groundwater management in drought-prone water-stressed Barind Tract, Bangladesh. *Environmental Challenges*, *4*, 100173. https://doi.org/10.1016/J.ENVC.2021.100173

Huete, A., Didan, K., Miura, T., Rodriguez, E. P., Gao, X., & Ferreira, L. G. (2002). Overview of the radiometric and biophysical performance of the MODIS vegetation indices. *Remote Sensing of Environment*, *83*(1–2), 195–213. https://doi.org/10.1016/S0034-4257(02)00096-2

Ishizaka, A., & Labib, A. (2011). Review of the main developments in the analytic hierarchy process. *Expert Systems with Applications*, *38*(11), 14336–14345. https://doi.org/10.1016/J.ESWA.2011.04.143

Jollife, I. T., & Cadima, J. (2016). Principal component analysis: A review and recent developments. *Philosophical Transactions of the Royal Society A: Mathematical, Physical and Engineering Sciences*, *374*(2065). https://doi.org/10.1098/RSTA.2015.0202/115142

Kamruzzaman, M., Almazroui, M., Salam, M. A., Mondol, M. A. H., Rahman, M. M., Deb, L., Kundu, P. K., Zaman, M. A. U., & Islam, A. R. M. T. (2022). Spatiotemporal drought analysis in Bangladesh using the standardized precipitation index (SPI) and standardized precipitation evapotranspiration index (SPEI). *Scientific Reports 2022 12:1*, *12*(1), 20694-. https://doi.org/10.1038/s41598-022-24146-0

Kim, J. E., Yu, J., Ryu, J. H., Lee, J. H., & Kim, T. W. (2021). Assessment of regional drought vulnerability and risk using principal component analysis and a Gaussian mixture model. *Natural Hazards 2021 109:1*, *109*(1), 707–724. https://doi.org/10.1007/S11069-021-04854-Y

Kogan, F. N. (1995). Application of vegetation index and brightness temperature for drought detection. *Advances in Space Research*, *15*(11), 91–100. https://doi.org/10.1016/0273-1177(95)00079-T

Kumar, K. K., Rajagopalan, B., & Cane, M. A. (1999). On the weakening relationship between the indian monsoon and ENSO. *Science*, *284*(5423), 2156–2159. https://doi.org/10.1126/SCIENCE.284.5423.2156;PAGEGROUP:STRING:PUBLICATION

Marufur Rahman, Md., & Q. M. Mahbub, A. (2012). Lithological Study and Mapping of Barind Tract Using Borehole Log Data with GIS: In the Context of Tanore Upazila. *Journal of Geographic Information System*, *04*(04), 349–357. https://doi.org/10.4236/JGIS.2012.44040

McPhaden, M. J., Zebiak, S. E., & Glantz, M. H. (2006). ENSO as an integrating concept in earth science. *Science*, *314*(5806), 1740–1745. https://doi.org/10.1126/SCIENCE.1132588;ISSUE:ISSUE:DOI

Mishra, A. K., & Singh, V. P. (2010). A review of drought concepts. *Journal of Hydrology*, *391*(1–2), 202–216. https://doi.org/10.1016/J.JHYDROL.2010.07.012

Mu, Q., Zhao, M., & Running, S. W. (2011). Improvements to a MODIS global terrestrial evapotranspiration algorithm. *Remote Sensing of Environment*, *115*(8), 1781–1800. https://doi.org/10.1016/J.RSE.2011.02.019

Naumann, G., Barbosa, P., Garrote, L., Iglesias, A., & Vogt, J. (2014). Exploring drought vulnerability in Africa: An indicator based analysis to be used in early warning systems. *Hydrology and Earth System Sciences*, *18*(5), 1591–1604. https://doi.org/10.5194/HESS-18-1591-2014

Park, S., Im, J., Jang, E., & Rhee, J. (2016). Drought assessment and monitoring through blending of multi-sensor indices using machine learning approaches for different climate regions. *Agricultural and Forest Meteorology*, *216*, 157–169. https://doi.org/10.1016/J.AGRFORMET.2015.10.011

Pekel, J. F., Cottam, A., Gorelick, N., & Belward, A. S. (2016). High-resolution mapping of global surface water and its long-term changes. *Nature 2016 540:7633*, *540*(7633), 418–422. https://doi.org/10.1038/nature20584

Prajapati, V. K., Khanna, M., Singh, M., Kaur, R., Sahoo, R. N., & Singh, D. K. (2022). PCA–based composite drought index for drought assessment in Marathwada region of Maharashtra state, India. *Theoretical and Applied Climatology 2022 149:1*, *149*(1), 207–220. https://doi.org/10.1007/S00704-022-04044-1

Quiring, S. M. (2009). Monitoring drought: An evaluation of meteorological drought indices. *Geography Compass*, *3*(1), 64–88. https://doi.org/10.1111/J.1749-8198.2008.00207.X;REQUESTEDJOURNAL:JOURNAL:17498198;JOURNAL:JOURNAL:17498198;ISSUE:ISSUE:DOI

Rahman, M. N., Rony, M. R. H., & Jannat, F. A. (2021). Spatiotemporal Evaluation Of Drought Trend During 1979–2019 In Seven Climatic Zones Of Bangladesh. *Heliyon*, *7*(11). https://doi.org/10.1016/j.heliyon.2021.e08249

Rahman, M. R., & Lateh, H. (2016). Meteorological drought in Bangladesh: assessing, analysing and hazard mapping using SPI, GIS and monthly rainfall data. *Environmental Earth Sciences 2016 75:12*, *75*(12), 1026-. https://doi.org/10.1007/S12665-016-5829-5

Rhee, J., Im, J., & Carbone, G. J. (2010). Monitoring agricultural drought for arid and humid regions using multi-sensor remote sensing data. *Remote Sensing of Environment*, *114*(12), 2875–2887. https://doi.org/10.1016/J.RSE.2010.07.005

Rodell, M., Houser, P. R., Jambor, U., Gottschalck, J., Mitchell, K., Meng, C.-J., Arsenault, K., Cosgrove, B., Radakovich, J., Bosilovich, M., Entin, J. K., Walker, J. P., Lohmann, D., Toll, D., Rodell, M., Houser, P. R., Jambor, U., Gottschalck, J., Mitchell, K., … Toll, D. (2004). The Global Land Data Assimilation System. *Bulletin of the American Meteorological Society*, *85*(3), 381–394. https://doi.org/10.1175/BAMS-85-3-381

Saaty, T. L. (2002). Decision making with the Analytic Hierarchy Process. *Scientia Iranica*, *9*(3), 215–229. https://doi.org/10.1504/IJSSCI.2008.017590

Sandholt, I., Rasmussen, K., & Andersen, J. (2002). A simple interpretation of the surface temperature/vegetation index space for assessment of surface moisture status. *Remote Sensing of Environment*, *79*(2–3), 213–224. https://doi.org/10.1016/S0034-4257(01)00274-7

Sarkar, S. K., Das, S., Rudra, R. R., Ekram, K. M. M., Haydar, M., Alam, E., Islam, M. K., & Islam, A. R. M. T. (2024). Delineating the drought vulnerability zones in Bangladesh. *Scientific Reports 2024 14:1*, *14*(1), 25564-. https://doi.org/10.1038/s41598-024-75690-w

Sattar, M. A., Mia, S., Shanta, A. A., Abdul Ahad Biswas, A. K. M., & Ludwig, F. (2021). Remote impacts from el niño and la niña on climate variables and major crops production in coastal bangladesh. *Atmosphere*, *12*(11), 1449. https://doi.org/10.3390/ATMOS12111449/S1

Schaaf, C. B., Gao, F., Strahler, A. H., Lucht, W., Li, X., Tsang, T., Strugnell, N. C., Zhang, X., Jin, Y., Muller, J. P., Lewis, P., Barnsley, M., Hobson, P., Disney, M., Roberts, G., Dunderdale, M., Doll, C., D'Entremont, R. P., Hu, B., … Roy, D. (2002). First operational BRDF, albedo nadir reflectance products from MODIS. *Remote Sensing of Environment*, *83*(1–2), 135–148. https://doi.org/10.1016/S0034-4257(02)00091-3

Shahid, S., & Behrawan, H. (2008). Drought risk assessment in the western part of Bangladesh. *Natural Hazards 2008 46:3*, *46*(3), 391–413. https://doi.org/10.1007/S11069-007-9191-5

Tahasin, A., Haydar, M., Hossen, M. S., & Sadia, H. (2024). Drought vulnerability assessment and its impact on crop production and livelihood of people: An empirical analysis of Barind Tract. *Heliyon*, *10*(20). https://doi.org/10.1016/j.heliyon.2024.e39067

Tucker, C. J. (1979). Red and photographic infrared linear combinations for monitoring vegetation. *Remote Sensing of Environment*, *8*(2), 127–150. https://doi.org/10.1016/0034-4257(79)90013-0

Van Loon, A. F. (2015). Hydrological drought explained. *Wiley Interdisciplinary Reviews: Water*, *2*(4), 359–392. https://doi.org/10.1002/WAT2.1085;WEBSITE:WEBSITE:WIRES;WGROUP:STRING:PUBLICATION

Vicente-Serrano, S. M., Beguería, S., López-Moreno, J. I., Vicente-Serrano, S. M., Beguería, S., & López-Moreno, J. I. (2010). A Multiscalar Drought Index Sensitive to Global Warming: The Standardized Precipitation Evapotranspiration Index. *Journal of Climate*, *23*(7), 1696–1718. https://doi.org/10.1175/2009JCLI2909.1

Wahiduzzaman, M., & Luo, J. J. (2020). A statistical analysis on the contribution of El Niño–Southern Oscillation to the rainfall and temperature over Bangladesh. *Meteorology and Atmospheric Physics 2020 133:1*, *133*(1), 55–68. https://doi.org/10.1007/S00703-020-00733-6

Wan, Z., Zhang, Y., Zhang, Q., & Li, Z. liang. (2002). Validation of the land-surface temperature products retrieved from Terra Moderate Resolution Imaging Spectroradiometer data. *Remote Sensing of Environment*, *83*(1–2), 163–180. https://doi.org/10.1016/S0034-4257(02)00093-7

Wilhite, D. A., & Glantz, M. H. (1985). Understanding: the Drought Phenomenon: The Role of Definitions. *Water International*, *10*(3), 111–120. https://doi.org/10.1080/02508068508686328

Zargar, A., Sadiq, R., Naser, B., & Khan, F. I. (2011). A review of drought indices. *Https://Doi.Org/10.1139/A11-013*, *19*(1), 333–349. https://doi.org/10.1139/A11-013